Academia Journal of Environmetal Science 4(2): 020-038, February 2016

DOI: 10.15413/ajes.2015.0600 ISSN: ISSN 2315-778X

©2016 Academia Publishing





Research Paper

Temporal and Spatial Changes in Climate Extremes and their Connection with Runoff in the Yellow River Basin between 1961 and 2010

Accepted 6th January, 2016

ABSTRACT

This study analyzes the temporal and spatial distribution of the extreme values of eight climate indices, based on observational data from a hundred and forty-three (143) meteorological stations across the basin. The eight core indices selected from the STARDEX projects reflect rather moderate extremes. The relationship between the eight indices and observed run-off from six hydrological stations was analyzed. Results showed that the annual and seasonal indices of temperature extremes for the period 1961 to 2010 increased most significantly for txq90, tnq10, and hxw90, which increased by about 0.8 to 1.3°C, 2.5 to 3.9°C, and 0.6 to 2.7 days, respectively, while the number of frost days decreased by 14.8 to 26.5 days. Sharp increases in txq90, trq10, and txhw90 occurred in the late 1980s and 1990s, and decreases in tnfd occurred in the 1990s. The rainfall extremes are significantly different to the temperature series between 1961 and 2010. From the result, no significant increasing or decreasing trends in rainfall extremes was observed. Out-of-phase variations in annual temperature extremes are evident between the middle and north-south regions, the west and east regions, and the northwest and southeast regions. The spatial distribution of rainfall also shows an out-of-phase pattern, but the trends are weaker than those of the temperature indices. Furthermore, the four temperature indices (txg90, tng10, tnfd and txhw90) and two of the rainfall indices (pnl90 and px5d) are more closely related to the observed run-off than the other two rainfall extremes.

Key words: Rainfall, temperature, extremes, run-off, temporal and spatial variation, Yellow River Basin.

C. Hu1*, J. Chen2, J. Niu2, F. He1 and J. Wang3

¹Department of Hydraulic Engineering, School of Water Conservancy and Environment Engineering, Zhengzhou University, No.100, Kexue Road, Zhengzhou City, P.R. China. ²Department of Civil Engineering, the University of Hong Kong, Pok Fu Lam Rd., Hong Kong, P.R. China. ³Henan Climate Center, No.100, Jinshui Road, Zhengzhou City, P.R. China.

Corresponding author e-mail: hucaihong@zzu.edu.cn. Tel: 18739919805.

INTRODUCTION

The variability and trends associated with extreme regional climate events, which can have significant social and economic impacts (directly or indirectly), have recently received much attention (Karl and Easterling, 1999; Easterling et al., 2000a; Meehl et al., 2000; Michele et al., 2004; Di et al., 2012; Emily et al., 2013). Normally, higher average air temperatures result in higher evaporation rates and increased atmospheric water vapor content. Consequently, an accelerated hydrological cycle develops (Menael and Bürger, 2002). Therefore, it is important to

understand how a changing climate could affect regional water supplies (Xu and Singh, 2004; Xu and Zhang, 2006; Zhang et al., 2009). Such studies must consider the frequency, intensity, and/or magnitude of extreme events that occurred in the past, as well as, possible future trends.

Much research into changes in climate extremes has been based on the analysis of climatic variables such as rainfall and temperature over daily time scales. Several studies have reported on the increased frequency of extreme climate events from China (Karl and Easterling, 1999; Easterling et al., 2000a, b; Alexander et al., 2006; Ding et al., 2010; Qin et al., 2010; You et al., 2010; Ren et al., 2011). The significant increase in the occurrence frequency of extreme temperatures in China is consistent with the global warming trend (Ding et al., 2010; Qin et al., 2010; You et al., 2010; Ren et al., 2012). Other studies have demonstrated that intense precipitation events, the total amount of precipitation, and maximum daily rainfall are increasing in most regions of southern China, but decreasing in northern China (Liu, 1999; Chen et al., 2005; Zhai et al., 2007).

As the 2nd largest river in China and the 6th largest river in the world, the Yellow River (95°53′E to 119°5′E; 32°10′N to 41°50′N) has been the subject of much research (Xu et al., 2007; Zhao et al., 2007; Tang et al., 2008; Zhang et al., 2008; Huang et al., 2009; Qin et al., 2010; Wang et al., 2012). Fu et al. (2004) found that the Yellow River watershed has become warmer, with a more significant increase in minimum temperature than in mean and maximum temperatures.

Wang and Qian (2009) showed that the entire basin is dominated by a significant increase in the frequency of warm days and nights, and increasing trends were found in temperature extremes (both maximum and minimum) over the period 1959 to 2008. You et al. (2010) demonstrated a significant upward trend in the frequency and intensity of high-temperature events observed at stations in the west and north of the Yellow River Basin, but not in the middle and lower Yellow River Basin. Approximately, the entire Yellow River Basin was dominated by a significant downward trend in the frequency of cold events (1960 to 2004).

The analysis of Hu et al. (2011) showed that significant warming trends have been observed over the whole Yellow River Basin between 1960 and 2006, and this warming is mainly related to a significant increase in minimum temperature. In contrast to the temperature indices, the indices related to extreme rainfall showed that changes in the precipitation indices are experiencing much weaker, or no significant changes from a basin-wide perspective (Xu and Zhang, 2006; Hu et al., 2011; Wang et al., 2012).

In addition, several studies indicated that run-off from the Yellow River decreased since the 1950s (Yang et al., 1998; Wang et al., 2006; Wang; and Li, 2011). A basic understanding of climate change and extremes was established in previous studies. However, the spatial and temporal heterogeneity of the trends in temperature and precipitation extremes and the factors driving these patterns remain unclear in the Yellow River Basin due to the complex spatial variations in climate and geomorphology. Therefore, a comprehensive study of a range of extreme variables will help to improve our understanding of these climate extremes and their relationship with run-off. This paper presents such a study, and investigates the changing patterns of climate extremes and their influence on run-off in the Yellow River Basin.

The objective of this study is to determine whether there

have been any statistically significant trends in temporal (annual to seasonal) and spatial changes in selected climate extremes indices, and in the influence of these indices on run-off, along the entire Yellow River. First, we will explore the trends in the climate extremes indices (txq90, tnq10, tnfd, txhw90, pq90, pnl90, px5d, and pint) between 1961 and 2010 and identify change points in the time series and associated statistical characteristics using linear regression and the Mann-Kendall (M-K) test. Then, the spatial change using empirical orthogonal function (EOF) analysis and wavelet analysis was considered. EOF analysis is used to compare the dominant patterns of temperature and rainfall extremes using temperature and rainfall records from the Yellow River Basin and the major modes of the outgoing long-wave radiation data for the period (1961 to 2010). Our analysis identified the characteristics of the spatial and temporal patterns of possible physical significance. The run-off recorded at six hydrological stations and its relationship with the climate extremes indices was also examined. We focused on the temporal trends in daily temperature and rainfall extremes, and the spatial patterns of extreme climate variability across the Yellow River Basin as well as, their influence on run-off.

Data

The Yellow River Basin is located in the north of central China, and is about 5464 km long with a drainage area of 752,400 km². The river originates on the eastern Qinghai—Tibet Plateau at an elevation of more than 5000 m, and then flows eastwards through the Loess Plateau and the North China Plain, before finally discharging into the Bohai Sea. There is considerable geological and climatic variability along the course of the Yellow River and it plays a key role in mainland China, where it is treated by the nation as the 'Mother River'. However, the river is affected by many serious issues, such as sedimentation, soil erosion, water shortages, and other environmental problems, and these issues have already restricted the sustainable development of the region.

The daily temperature data (including maximum, mean, and minimum) and daily rainfall data obtained from 143 meteorological stations (Figure 1) for the period 1961 to 2010 (provided by the Henan Climate Center) were used to calculate the extreme indices. To facilitate this study and provide a brief overview of the climate in the study region, the upper, middle, and lower reaches of the Yellow River Basin were divided (Figure 1). Accordingly, 53 meteorological stations were located in the upper section, 78 stations in the middle section, and 12 stations downstream. The homogeneity of the daily temperature and rainfall series data has been demonstrated by the Henan Climate Center, at a significance level of 95%. Annual data for 6 hydrological stations (at Lanzhou, Toudaoguai, Longmen, Sanmenxia, Huayuankou, and Lijin; Figure 1) located in the upper, middle, and lower regions, were also used to increase the robustness of the analysis.

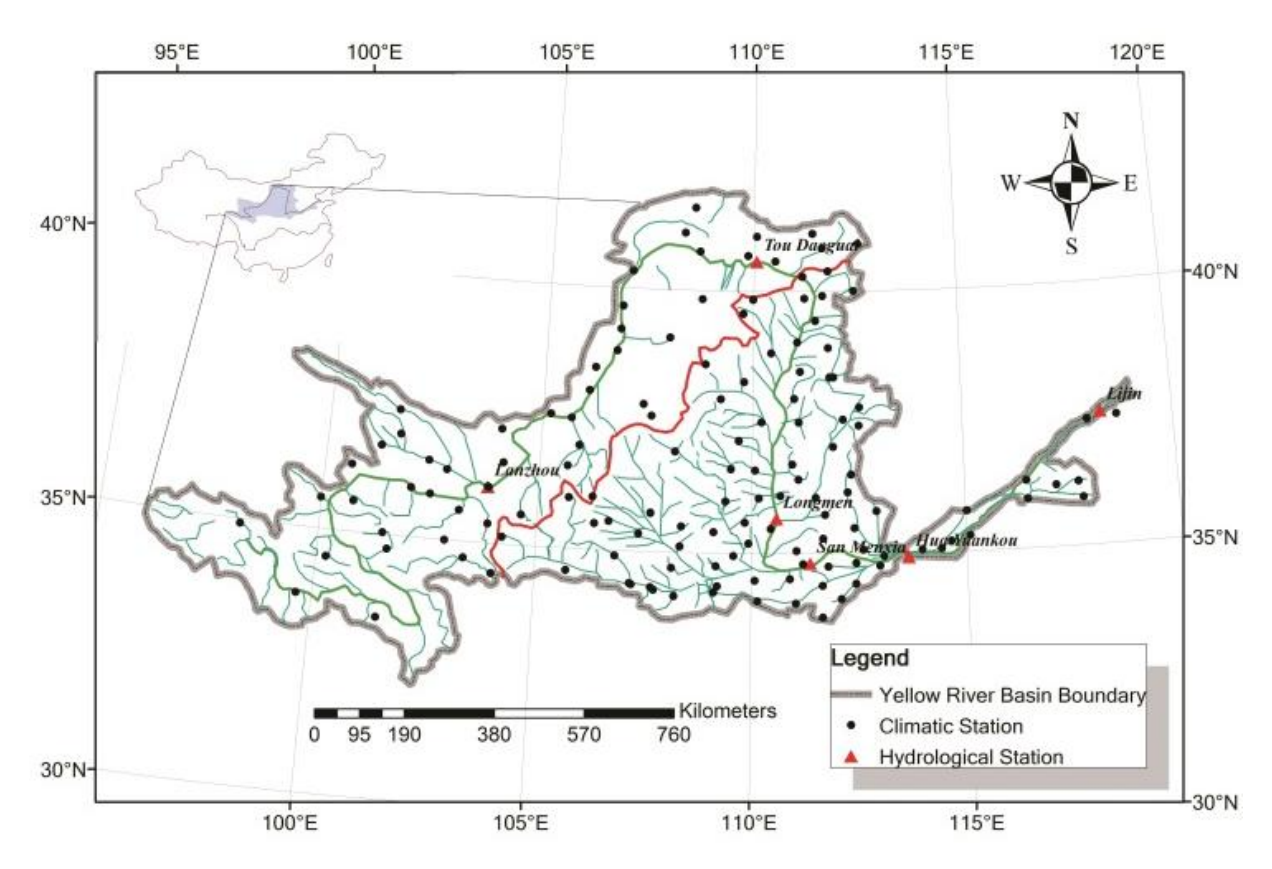


Figure 1. Map showing the study area in China and locations of gauging stations.

Table 1. The eight key weather and climate indices used in this study.

S/No.	Index code	User friendly name	Description			
	Temperatur	e indices				
1	txq90	Hot-day threshold	Tmax 90 th percentile (°C)- the 10th hottest day per season			
2	tnq10	Cold-night threshold	T min 10 th percentile (°C) – the 10th coldest night per season			
3	tnfd	Frost days	Number of frost days T min < 0 °C			
4	txhw90	Longest heat wave	Heat wave duration (days)			
	Rainfall ind	ices				
5	pq90	Heavy rainfall threshold	90 th percentile of rain day amounts (mm/day)			
6	pnl90	Heavy rainfall days	Number of events > long-term 90 th percentile of rain days			
7	P×5d	Greatest 5-day rainfall (amount)	Greatest 5-day total rainfall (mm)			
8	pint	Average wet-day rainfall (amount)	Simple daily intensity (rain per rain day) (mm/day)			

METHODOLOGY

3.1. Indices of Climate Extremes and Statistical Testing

The STARDEX (statistical and regional dynamical downscaling of extremes for European regions) indices of extremes are defined from a climatic perspective. Eight key indices extracted from the STARDEX project (http://www.cru.uea.ac.uk/cru/projects/stardex/, 2004) were used to analyze climate extremes over the Yellow River Basin. The indices shown in Table 1 were used in this

study to represent climate extremes as evaluation criteria to examine the extreme events. These key indices cover the magnitude (for example, hot-day and heavy-rainfall thresholds), frequency (for example, frost days and heavy rainfall days), and persistence (for example, greatest 5-day total rainfall and longest heatwave) of climate extremes. All of the indices were derived from daily maximum and minimum temperature, and daily rainfall data. The eight selected indices ensured that the annual number of extremes was sufficiently high to allow meaningful trend

analysis of the selected data series, which was 50 years long (1961 to 2010). Furthermore, the indices chosen reflect changes in moderately strong events (rather than highly unusual events) to ensure robustness as regards to the detectability of trends (Frei and Schär, 2001; Klein and Können, 2003; Chen et al., 2010). However, rainfall indices, including pq90, pnl90, pint, and px5d, were separated into wet and dry days, where a wet day (dry day) was defined as a day with at least 1.0 mm (less than 1.0 mm) of rainfall.

MATERIALS AND METHODS

Both simple linear regression and the M-K test were used to quantify the magnitude of the overall trends in the indices of temperature and rainfall extremes and other variables. The linear regression method was selected to test the long-term trends because of its simplicity when dealing with an unknown trend. The rank-based M-K test is a nonparametric method, widely applied to the analysis of changing processes and the change points meteorological and hydrological variables through time (Mann, 1945; Kendall, 1975; Ma and Fu, 2003; Yue and Pilon, 2004; Partal and Kahya, 2006; Zhang et al., 2008; Wang and Li, 2011). Both the linear regression and M-K methods have been widely used to assess trends and their significance in hydrometeorogical time series, especially in recent studies of climate extremes (Gemmer et al., 2011; Vincent et al., 2011). In this study, before the M-K test was applied, the extreme series were tested using linear regression. Statistical significance was taken as the 95% confidence level. The M-K test was used to assess the significance level. This paper investigates whether eight variables associated with the climate extremes and discharge records of the Yellow River exhibit evidence of change, either gradual changes (trend) or sharp changes (jump) during the period 1961 to 2010 using the M-K test. Both methods are commonly used to assess the significance of trends in hydro-meteorological time series, and most recently, particularly with respect to climate extremes (e.g., Vincent et al. 2011; Gemmer et al., 2011; Yang et al., 2011).

In addition, spatial patterns in the indices of temperature and rainfall extremes were detected in this study using the sequential version of empirical orthogonal function (EOF) analysis (Keiner and Yan, 1997; Lee et al., 2003; Mohapatra et al., 2003; Singh, 2004), which is widely used to study spatial patterns in various meteorological parameters. EOF was used to investigate the dominant spatial patterns of the indices of temperature and rainfall extremes, and to identify the homogenous regions in the Yellow River Basin. The EOF method is a statistical technique that can be used to estimate both the patterns of physical processes (spatial variability) and the time series coefficients modulating each process (temporal variability) by decomposing a multivariate data set into an uncorrelated linear combination of separate functions of the original variables. The eigenvectors, one of the outputs of the EOF method, are plotted as vector maps to describe spatial variability by showing the regions that are closely related, either directly or inversely. The error range of the eigenvector values presented by North et al. (1982) was used in the significance testing. The wavelet analysis method (Compagnucci et al., 2000; Prokoph and Patterson, 2004; Labat, 2005; Villoria et al., 2012) is a powerful method for analyzing a time series over different periods and frequencies, and identifying its principal components.

RESULTS AND DISCUSSION

Temporal trends and distribution of climate extremes

Using linear regression and the M-K test, significant differences in the daily temperature and rainfall extremes were found in the three sub-regions of the Yellow River Basin (Figure 2 (a) to (h)). The change trends in the daily indices of climate extremes at the 143 meteorological stations are shown in Figure 3 (a) to (h). Table 2 summarizes the trends of the four indices of seasonal and annual temperature and highlights their abrupt changes between 1961 and 2010, while Table 3 shows trends and station numbers at the 95% significance level of the seasonal and annual rainfall indices and their change points for the period 1961 to 2010.

Temperature indices

The trend in the hot-day threshold (txg90) showed a statistically significant (95% level) increase by 0.8°C and 1.3°C during the period 1961 to 2010 in the upper and middle regions, respectively, while it decreased by 0.6°C in the lower region (Figure 2a and Table 2). A sharp increase is seen around 2000, 1999, and 1971 in the upper, middle, and lower regions, respectively. Analysis of the annual txq90 series showed a spatially coherent increase at 48.3% (69) of the stations, which was significant at the 95% level and concentrated mainly across the upper and middle zones (Figure 3a and Table 2). Meanwhile, two and four stations showed negative trends in the middle and downstream reaches, respectively. On a seasonal basis, txq90 followed a well-defined increasing trend in winter and autumn, with 86.0% (123 stations) and 76.9%(110 stations) of the stations for the period 1961 to 2010. From 1961 to 2010, txg90 increased by 2.5 to 1.6°C from the upper to the downstream sections in winter, and by 2.1 to 1.4°C in autumn. However, in the downstream region, the range of changes decreased by 0.6 and 0.7°C in the spring and summer, respectively (Table 2). Similarly, a significant increasing trend also dominated 37.8% (54 stations) and 53.1% (76 stations) of all stations in spring and summer, respectively, while there were six and one station with significant negative trends sparsely distributed in the



Figure 2. Regional annual series for indices of eight extremes in the Yellow River Basin.

middle and downstream sections, respectively, for the period 1961 to 2010.

The indices tnq10 and txhw90 showed statistically significant increases by 2.5 to 3.9°C and 1.4 to 2.7°C, respectively, between 1961 and 2010 in the three subregions, with sharp increases in tnq10 occurring in the late 1980s in all three subregions and in txhw90 in the early 2000s in the upper region (Table 2 and Figure 2b and d). Most stations showed a statistically significant increasing trend, and only a few stations had a significant negative trend (Figure 3b, d and Table 2). The detailed characteristics of tnq10 and txhw90 are shown in Table 2 and Figures 2

and 3. Furthermore, the magnitude of increase in tnq10 was much larger than that in the txq90, and comparable with txhw90 over both the annual and seasonal timescales. The decrease in the number of frost days (tnfd) also showed statistically significant trends (Figure 2c, d and Table 2). The analysis of tnfd at the annual scale showed a statistically significant negative trend at 81.8% (117) of the stations (Figure 3c, d). The largest changes occurred in the upper and lower zones at 96.9% (139) of the stations, with a large proportion of stations showing a significant decrease during winter and spring (66.4 and 72.0%, respectively) between 1961 and 2010.

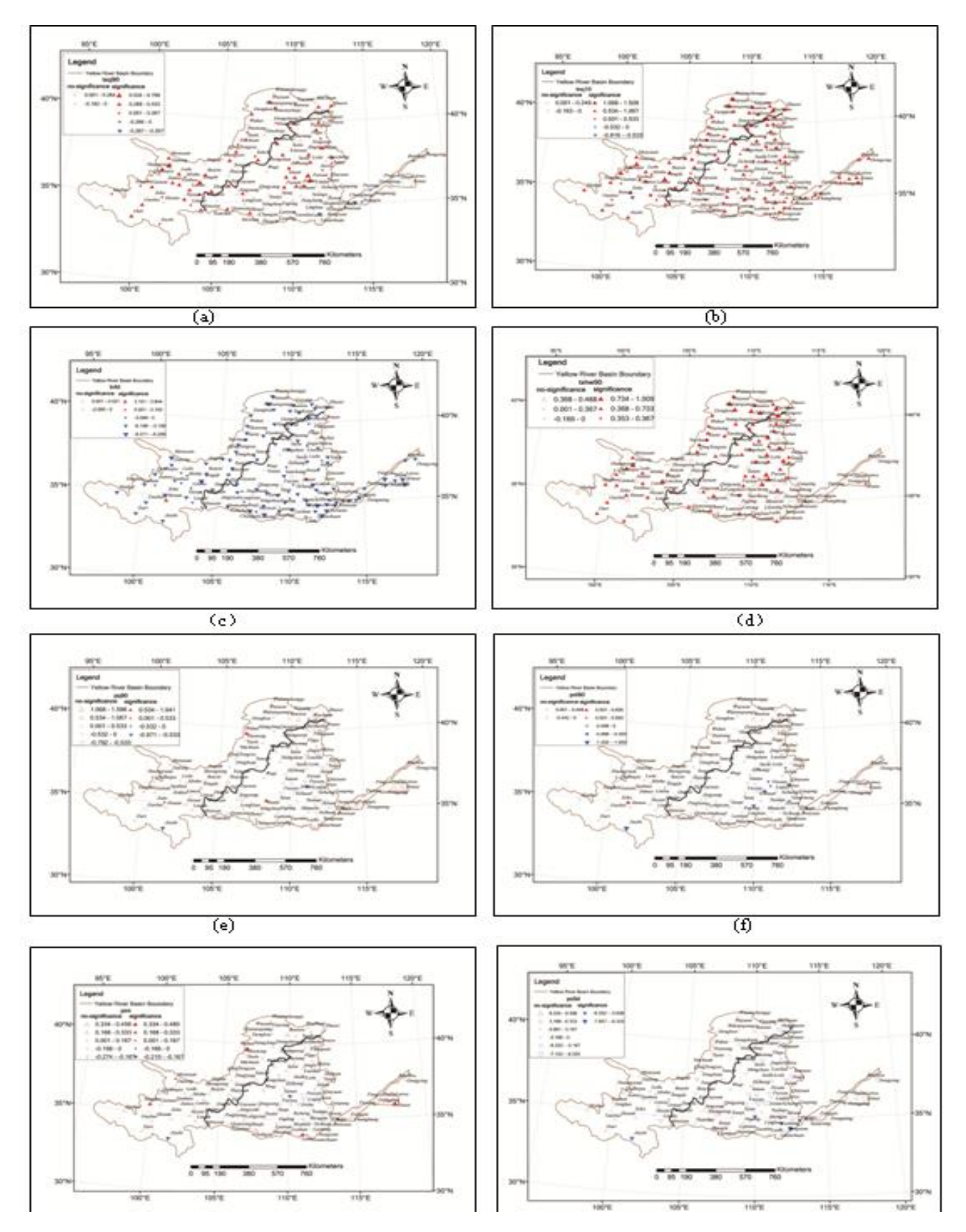


Figure 3. Timing of change at the stations for eight indices of climate extremes across the Yellow River Basin: red upward-pointing triangles indicate a significant increase; blue downward-pointing triangles indicate a significant increase.

Table 2. Trends of seasonal and annual txq90, tnq10, tnfd, and txhw90, and their abrupt changes over the period 1961 to 2010.

Sub- region	Index	Season	Change rate /(/10 a)	Abrupt year	Change magnitude during 50 years	Average during 50 years	Stations at the level 95% significance
		Winter	+0.51***	1997(+)	2.5	6.4	(+)50, (-)0
		Spring	0.15	2002(+)	0.8	23.2	(+)13, (-)0
	txq90/°C	Summer	+0.3***	1997(+)	1.5	28.5	(+)42, (-)0
		Autumn	+0.41***	2002(+)	2.1	21.6	(+)46, (-)0
		Annual	+0.26***	2000(+)	1.3	25.9	(+)40, (-)0
		Winter	+0.7***	1986(+)	3.4	-19.4	(+)49, (-)1
		Spring	+0.54***	1990(+)	2.7	-7.5	(+)44, (-)0
	tnq10°C	Summer	+0.53***	1990(+)	2.7	7.8	(+)51, (-)0
		Autumn	+0.46***	1994(+)	2.3	-8.9	(+)34, (-)0
		Annual	+0.77***	1986(+)	3.9	-15	(+)52, (-)1
Jpstream		Winter	-0.18***	/	-0.9	90	(+)0, (-)22
pourum			-0.18 -2.05***	,			
		Spring		1989(-)	-10.3	44	(+)0, (-)45
	tnfd/days	Summer	-0.54***	1973- 1976(-)	-2.7	3	(+)0, (-)18
		Autumn	-1.35***	1994(-)	-6.8	43.8	(+)1, (-)34
		Annual	-4.11***	1992(-)	-20.6	180.8	(+)1, (-)51
		Winter	+0.52***	2005(+)	2.5	3.2	(+)41, (-)0
		Spring	+0.27***	2002- 2005(+)	1.4	3	(+)33, (-)0
	txhw90/days	Summer	+0.46***	2004(+)	2.3	3.2	(+)26, (-)0
		Autumn	+0.34***	2003(+)	1.7	3.2	(+)31, (-)0
		Annual	+0.53***	2008(+)	2.7	5.1	(+)37, (-)0
		Winter	+0.49***	1993(+)	2.4	9.6	(+)69, (-)0
		Spring	+0.31**	/	1.6	27.6	(+)40, (-)0
	txq90/°C	Summer	+0.17**	/	0.9	33.1	(+)34, (-)4
	unqs or e	Autumn	+0.37***	1986(+)	1.9	25.4	(+)56, (-)0
		Annual	+0.16**	1999(+)	0.8	30.4	(+)29, (-)2
		Winter	+0.44***	1981(+)	2.2	-13.1	(1)51 (1)0
			+0.44 +0.32***				(+)51, (-)0
	tm a 100C	Spring	+0.32	1996(+)	1.6	-2.6	(+)35, (-)0
	tnq10°C	Summer		1992(+)	1.5	13.5	(+)53, (-)2
		Autumn	0.12	2002(+)	0.6	-3.5	(+)17, (-)2
Midstroom		Annual	+0.5***	1988(+)	2.5	-9.2	(+)65, (-)0
Midstream		Winter	-1.41***	1992(-)	-6.9	84.1	(+)0, (-)61
		Spring	-1.23***	1995(-)	-6.2	20.7	(+)1, (-)46
	tnfd/days	Summer	0	/	0	0	(+)0, (-)3
		Autumn	-0.35	/	-1.8	22.2	(+)3, (-)19
		Annual	-2.95***	1996(-)	-14.8	127	(+)1, (-)54
		Winter	+0.52***	1997(+)	2.5	3.2	(+)62, (-)0
		Spring	+0.31***	2004(+)	1.6	3	(+)47, (-)0
	txhw90/days	Summer	0.19	2004(±) /	1.0	3.2	(+)47, (-)0 (+)19, (-)2
	MIW 70/days		0.19		1.6		
		Autumn		1007(.)		3.3	(+)40, (-)0
		Annual	+0.45**	1997(+)	2.3	5.2	(+)37, (-)0

Table 2 contd. Trends of seasonal and annual txq90, tnq10, tnfd, and txhw90, and their abrupt changes over the period 1961 to 2010.

		Winter	+0.33**	1993(+)	1.6	11.4	(+)4, (-)0
		Spring	-0.11	1974(-)	-0.6	29.2	(+)1, (-)1
	•	Summer	-0.13	1973(-)	-0.7	34.8	(+)0, (-)2
		Autumn	+0.27***	1988(+)	1.4	28.5	(+)8, (-)0
		Annual	-0.12*	1971(-)	-0.6	32.3	(+)0, (-)4
		Winter	+0.65***	1986(+)	3.2	-9	(+)11, (-)0
		Spring	+0.58***	1994(+)	2.9	0.1	(+)12, (-)0
	tnq10°C	Summer	+0.26***	1991(+)	1.3	17.8	(+)8, (-)0
	•	Autumn	0.16	2002(+)	0.8	0.1	(+)5, (-)0
		Annual	+0.59***	1989(+)	3	-5.3	(+)12, (-)0
Downstream							
		Winter	-2.94***	1989(-)	-14.4	78	(+)0, (-)12
		Spring	-1.8***	1989(-)	-9	10.1	(+)0, (-)12
	tnfd/days	Summer	0	/	0	0	(+)0, (-)0
		Autumn	-0.6	1997(-)	-3	9.6	(+)0, (-)6
		Annual	-5.29***	1992(-)	-26.5	97.7	(+)0, (-)12
		Winter	0.16	/	0.8	3.1	(+)0, (-)0
		Spring	0.13	/	0.7	2.9	(+)1, (-)0
	txhw90/days	Summer	-0.23*	/	-1.2	2.8	(+)0, (-)4
	•	Autumn	0.22	/	1.1	3.3	(+)2, (-)0
		Annual	0.12	/	0.6	4.7	(+)1, (-)0

^{***, **,} and * indicate trends significant at the 99, 95 and 90% levels, respectively.

Table 3. Trends in seasonal and annual pq90, pnl90, pint, and px5d, and their abrupt changes over the period 1961 to 2010.

Sub- stream	Index	Season	Change rate//10a	Abrupt year	Change magnitude during 50yr	Average during 50yr/	Stations at the level 95% significance
		Summer	0.03	1992(+)	0.2	17.5	(+)2, (-)1
	pq90/mm	Annual	0.17	1994(+)	0.9	14.7	(+)2, (-)1
	100/1	Summer	-0.01	/	-0.1	2.5	(+)2, (-)1
	pnl90/days	Annual	0.02	/	0.1	5.2	(+)1, (-)1
Upstream	Pint/mm/day	Summer	0.06	1993- 1994(+)	0.3	7.9	(+)0, (-)0
		Annual	0.04	/	0.2	6.5	(+)3, (-)1
		Summer	-0.68	/	-3.4	51	(+)0, (-)1
	p ×5d/mm	Annual	-0.52	/	-2.6	53.9	(+)0, (-)2
	m a 00 /mm	Summer	-0.03	1975(-)	-0.2	26.3	(+)1, (-)1
	pq90/mm	Annual	-0.04	/	-0.2	20.8	(+)1, (-)1
	nn100/days	Summer	-0.03	/	-0.2	2.4	(+)2, (-)4
Midstream	pnl90/days	Annual	-0.16	/	-0.8	5.8	(+)0, (-)9
	pint/mm/day	Summer	0.07	1975(+)	0.4	11.4	(+)7, (-)0
	Pintininiday	Annual	-0.01	1993(-)	-0.1	8.9	(+)1, (-)1

Table 3 contd. Trends in seasonal and annual pq90, pnl90, pint, and px5d, and their abrupt changes over the period 1961 to 2010.

-							
	px5d/mm	Summer	-0.7	1983-1984(-)	-3.5	81.6	(+)0, (-)1
	px3u/IIIII	Annual	-1.89	1983(-)	-9.5	89	(+)0, (-)4
		Summer	0.61	2001(+)	3.1	41.2	(+)0 ()0
	pq90/mm	Summer		` /			(+)0, (-)0
	Parsimin	Annual	0.86^{*}	1993(+)	4.3	31	(+)0, (-)0
	mm100/dovis	Summer	0.04	/	0.2	2.2	(+)0, (-)0
	pnl90/days	Annual	0.05	/	0.3	4.9	(+)0, (-)0
Downstream							
	Pint/mm/day	Summer	0.17	/	0.9	17.2	(+)0, (-)0
	r iiii/iiiii/day	Annual	0.23	1993-1994(+)	1.2	12.4	(+)1, (-)0
	py5d/mm	Summer	-1.74	/	-8.7	123.1	(+)0, (-)0
	px5d/mm	Annual	-0.97	/	-4.9	128.7	(+)0, (-)0

^{***, **,} and * indicate trends significant at the 99, 95 and 90% levels, respectively.

There was increase in txq90, tnq10, and txhw90, and decrease in tnfd which indicated that extreme values of temperature followed a warming trend. This is consistent with the trend in the global diurnal temperature range (Eastering et al., 2000b). It is worth noting that the warming trends over the study area during the period 1961 to 2010 are similar to those reported by Hu et al. (2012) in the source region, Li et al. (2010) in the middle region, and Zhang et al. (2008) and Wang et al. (2012) for the Yellow River. However, variations exist in the temporal and spatial trends of the extreme climate indicators, as few studies have examined the trends in extreme climate events in the Yellow River Basin caused by differences in terms of the time period studied and the number of stations used. For example, Hu et al. (2012) reported many stations with increasing trends in txq90 over the period 1961 to 2006, with as many as 70% of all stations (14) showing statistically significant trends in the upper section as compared with 75.5% (40 stations) of all stations (53 stations) during the period 1961 to 2010 in this study. For the middle region, Li et al. (2010) found a significant trend in txq90 at 50% of the stations (increased by 0.02°C/year; 50 stations), in tnfd for 80% of the stations (decreased by 0.41 days/year), in txhw90 for about 90% of the stations (increased by 0.09 days/year), and in tnq10 for 98% of the stations (increased by 0.07°C/year). The threshold of temperature extremes (txq90 and tnq10) increased, while hot (txhw90)/cold (tnfd) extremes tended to be prolonged or shortened. However, in our study, there was a significant trend in txg90 at 37.2% of the stations (increased by 0.016°C/year) (78 stations), in tnfd at 69.2% of the stations (decreased by 0.296 days/year), in txhw90 at about 47.4% of the stations (increased by 0.046 days/year), and in tnq10 at 83.3% of the stations increased by 0.05°C/year.

Rainfall indices

In contrast to the temperature indices, rainfall indices showed weakly significant increasing and decreasing trends during 1961 to 2010. Linear regression and the M-K test showed that about 2.1% (3 stations), 3.5% (5 stations), and 0.7% (1 station) of all stations followed an upward trend (at a significance level of 95%) in the annual series of pq90 (heavy rainfall threshold), pint (average wet-day rainfall amount), and pnl90 (heavy rainfall days), respectively (Table 3). A downward trend was found in 1.4, 4.2, 1.4, and 7.0% of all stations for pq90, px5d (greatest 5day rainfall amount), pnl90, and pint, respectively (Figure 3e to h and Table 3). Significant trends in the four rainfall indices were only found at a few stations, and these were widely spread across the Yellow River Basin, but nonsignificant trends were found at most stations. From Table 3 and Figure 3, it can be seen that no coherent spatial patterns are evident in the indices of rainfall extremes, with many mixed positive, negative, and no-change sites spread across the entire basin, especially in the upper and middle sections. Meanwhile, there are large differences in the spatial distributions of the trends in indices of rainfall extremes from the different regions. Figure 2e to h shows the annual trends in precipitation extremes. The heavy rainfall threshold (pq90) changed slightly, increasing at a rate of 0.17 mm/decade and 0.86 mm/decade in the upper and lower reaches, respectively, and with rate of decrease of 0.03 mm/decade in the middle section (Table 3). The trend for the period 1961 to 2010 of both pnl90 and pint was also slightly increasing in the upper and downstream sections, but decreasing in the middle section. For px5d, the trend was slightly decreasing, at a rate of 0.52 mm/decade, 1.89 mm/decade, and 0.97 mm/decade in the upper, middle,

Table 4. The variance explained by the EOFs for indices of temperature extremes.

EOF	txq90		tnq10			tnfd	tx	txhw90	
No.	Variance (%)	Cumulative total variance (%)	Variance (%)	Cumulative total variance (%)	Variance (%)	Cumulative total variance (%)	Variance (%)	Cumulative total variance (%)	
EOF_1	53.50*	53.50*	56.75*	56.75*	45.23*	45.23*	49.17*	49.17*	
EOF_2	13.04*	66.54*	13.23*	69.98*	14.86*	60.09*	11.89*	61.06*	
EOF ₃	9.05*	75.59*	6.14*	76.13*	7.39*	67.48*	6.75*	67.81*	

^{*} indicates significant in the North test.

Table 5. The variance explained by the EOFs for indices of rainfall extremes.

Indices	Variance (%)	EOF ₁	EOF ₂	EOF ₃	EOF ₄	EOF ₅	EOF ₆	EOF ₇	EOF ₈	EOF ₉	EOF ₁₀
	Variance	16.83 *	10.80 *	7.75 *	7.03	6.26	5.29	4.95	4.21 *	3.20 *	2.91
pq90	Cumulative total variance	16.83 *	27.63 *	35.38 *	42.41	48.67	53.96	58.91	63.12 *	66.31 *	69.22
	Variance	21.21 *	10.30 *	7.34 *	6.37 *	4.92 *	4.49	4.28 *	3.41 *	3.22	3.00 *
pnl90	Cumulative total variance	21.21 *	31.51 *	38.86 *	45.23 *	50.15 *	54.64	58.92 *	62.34 *	65.56	68.56 *
	Variance	17.23 *	11.97 *	7.60 *	6.76	6.07	5.15	4.42	4.08	3.42	2.92
px5d	Cumulative total variance	17.23 *	29.20 *	36.80 *	43.56	49.63	54.78	59.2	63.28	66.7	69.62
	Variance	17.50 *	10.81 *	9.19 *	7.04 *	6.08	5.64	4.58	3.84 *	2.98 *	2.76
pint	Cumulative total variance	17.50 *	28.32 *	37.50 *	44.54 *	50.63	56.26	60.85	64.69 *	67.67 *	70.43

^{*} indicates significant in the North test.

and downstream sections, respectively. These results display various spatial variations. Weakly decreasing trends in the middle section, and slightly increasing trends in the upstream and downstream sections, were identified for pq90, pnl90, and pint. Insignificant change in annual rainfall was also reported previously for the Yellow River or its source region (Fu et al., 2004; Xu et al., 2007; Zhao et al., 2007; Hu et al., 2011).

Comparing the top, middle, and bottom rows of Figure_2 (except txhw90 and pnl90) it can be seen that changes in the value of the indices followed a multistep pattern moving from upstream to downstream. Figure 3 shows that the spatial variation is significant, which reflects the spatial and seasonal variations of changes in temperature and rainfall extremes. Obvious changing trends were observed in the temperature extremes indices but not for the rainfall indices across the whole basin from the mixed spatial pattern of significant and insignificant change in Tables 2

and 3 and Figure 3.

Spatial distributions and pattern of climate extremes

The indices of temperature and rainfall extremes are spatially variable in the Yellow River Basin. EOF analysis was performed on the indices of annual temperature and rainfall extremes to further explore these spatial variations. Tables 4 and 5 show the percentage of variance explained (in decreasing order) by various principal components for the temperature and rainfall data. As can be seen, the principal components up to levels 3 and 10 explained more than 67.48% of the variance for the temperature and rainfall extremes indices, respectively. Figures 4, 5, 6 and 7 showed the first, second, and third principal components and the percentage of total variance explained.

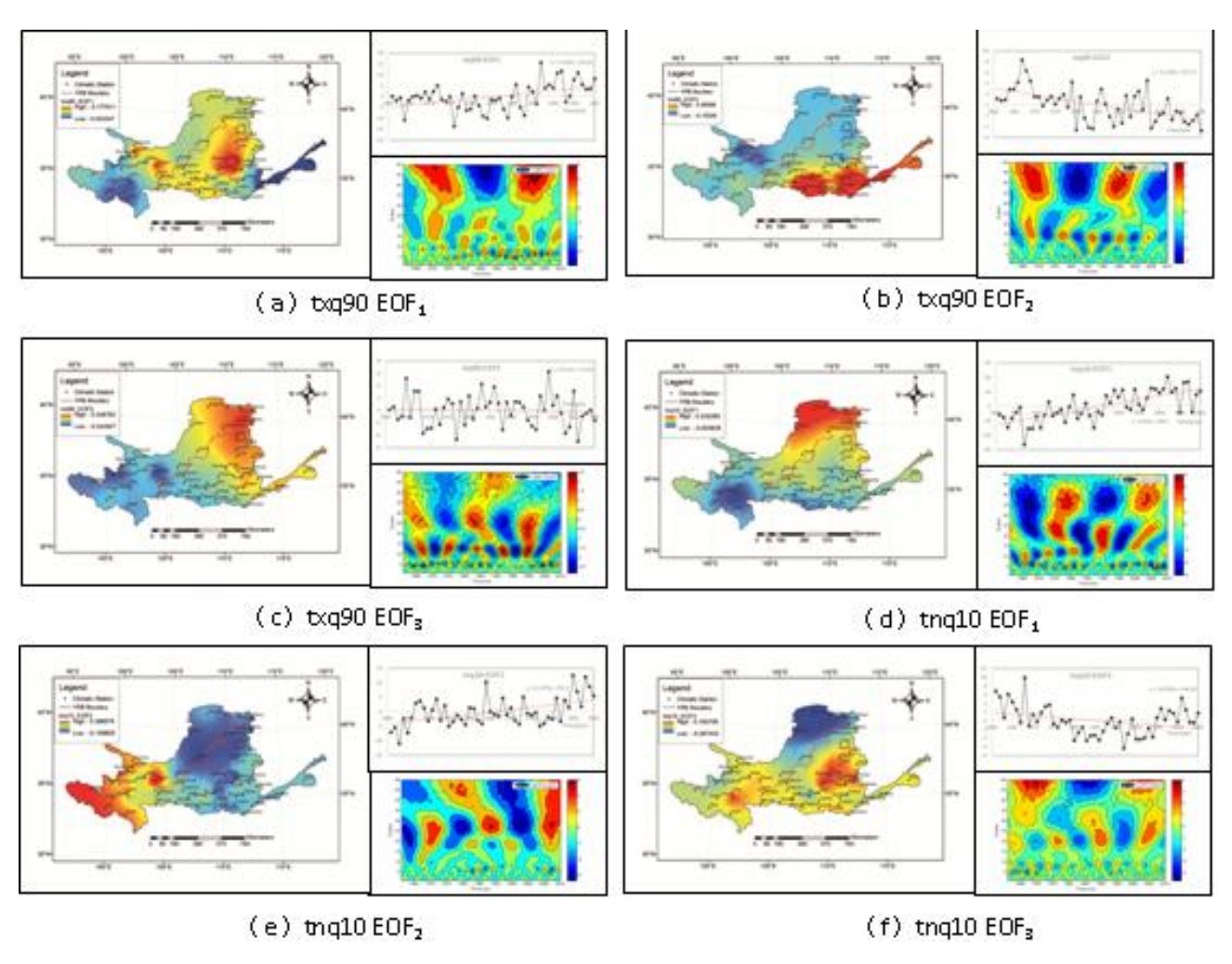


Figure 4. Spatial distribution of EOF1-3 for indices of temperature extremes (txq90 and tnq10), coefficient change trends, and wavelet transform of time series in the Yellow River Basin.

Temperature indices

Table 4 and Figure 4a showed the first principal component and the percentage of total variance explained. For txq90, tnq10, tnfd, and txhw90, the first principal component explains 53.50, 56.75, 45.23 and 49.17% of total variance, respectively. In addition, the accumulated variance for these three principal components accounts for over 65% of the total variance for these four temperature indices. This indicates that the spatial pattern of temperature extremes over the Yellow River was statistically significant at the annual scale. The four indices of temperature extremes exhibit different spatial patterns to each other.

As an example, for txq90 (Figure 4a to c and Table 4), the variances of EOF_1 , EOF_2 , and EOF_3 were 53.5, 13.04 and 9.05%, respectively, and their cumulative total variances were 53.5, 66.54 and 75.59%, respectively, at the significant North level (North et al., 1982). The change in variance between the first and second spatial variance

modes was also very large; indicating that txq90 in the Yellow River Basin was dominated by a unique spatial pattern. This implies that the eigenvalues of temporal and spatial variances were similar to each other. Figure 4a shows an obvious out-of-phase pattern for EOF_1 between the middle, and east-west regions, which indicates a decreasing trend from the middle to the east and west, or a decreasing trend from the east and west to the middle, across the whole Yellow River Basin.

High values of this mode are distributed along the border between Shanxi and Shannxi provinces; that is, in Shenmu County (ShannXi Province), Xixian County (Shanxi Province), and Baoji city in Shannxi Province. This also suggests that these areas are vulnerable to high temperatures. The distribution pattern (Figure 4b) of EOF_2 shows an out-of-phase relationship between the southeast and northwest, which means that txq90 in the south-east is high, but low in the northwest, and vice versa. The distribution pattern (Figure 4c) of EOF_3 is out-of-phase between the northeast and southwest, and changes from

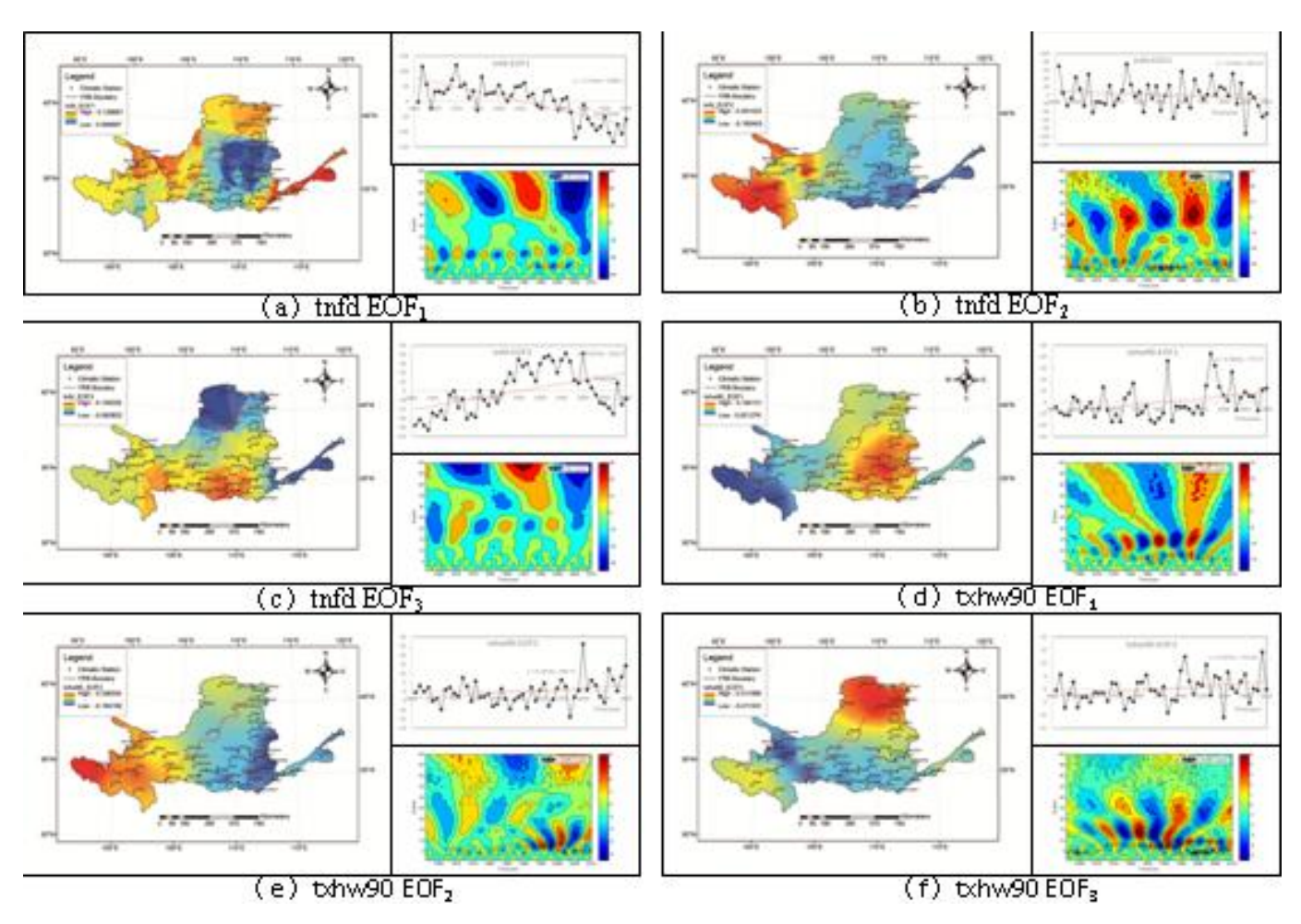


Figure 5. Spatial distribution of EOF1-3 for rainfall index (pq90), coefficient change trends, and wavelet transform of time series in the study area.

high values near the border of Shanxi and Shannxi provinces with the Inner Mongolia Autonomous Region in the northeast of the basin, to low values around Tongde and Xinghai counties in Qinghai Province in the southwest. EOF₁ describes the main distribution pattern for txq90. These modes appear to reflect the typical spatiotemporal characteristics of the distribution of txq90. Our analysis of the coefficient of EOF₁ for txq90 between 1961 and 2010 showed a significant increasing trend with a rate of 1.895/decade (Fig. 4 (a)). The value of the time coefficient of EOF₁ was mainly negative before 1990, but mainly positive after 1990. Therefore, the time series of txq90 shows larger values in the middle regions, but lower values in the east and west after 1990, which means that txq90 followed a significant increasing tendency in the middle region. The coefficient of EOF₂ for txq90 between 1961 and 2010 showed a significant decreasing trend of 1.195/decade (Figure 4b). For EOF₃ of txq90, the coefficient showed a significant increasing trend, with a rate of 0.115/decade (Figure 4c). Over the whole time domain of txq90, interannual cycles were evident with periods of 6 years (EOF₁), 14 and 25 years (EOF₂), and 4 and 25 years (EOF_3), indicating the presence of notable interannual cyclicity throughout the period of wavelet analysis (Figure 4a to c).

From Table 4 and Figure 4d to f), it can be seen that the variances of EOF₁, EOF₂, and EOF₃ for tnq10 were 56.75, 13.23, and 6.14%, respectively, and their cumulative total variances were 56.75, 69.98 and 76.13%, respectively, at the significant North level (North et al., 1982). The first, second, and third modes decomposed using the EOF method show out-of-phase patterns for the northeastand southwest, east-west, north-south respectively. Among them, EOF1 shows a decreasing trend from the high values in Wuyuan County (Inner Mongolia Autonomous Region) in the northeast to the low values in Henan County (Qinghai Province) in the southwest of the Yellow River Basin. The analysis of the coefficient of EOF₁ for tng10 between 1961 and 2010 shows a significant increasing trend at the rapid rate of 5.03/decade. The coldnight threshold (tnq10) shows significant increases in the north of the Yellow River Basin after 1990. The coefficient of EOF2 shows an increasing tendency at a rate of 1.697/decade. EOF₃ was found to have higher values in

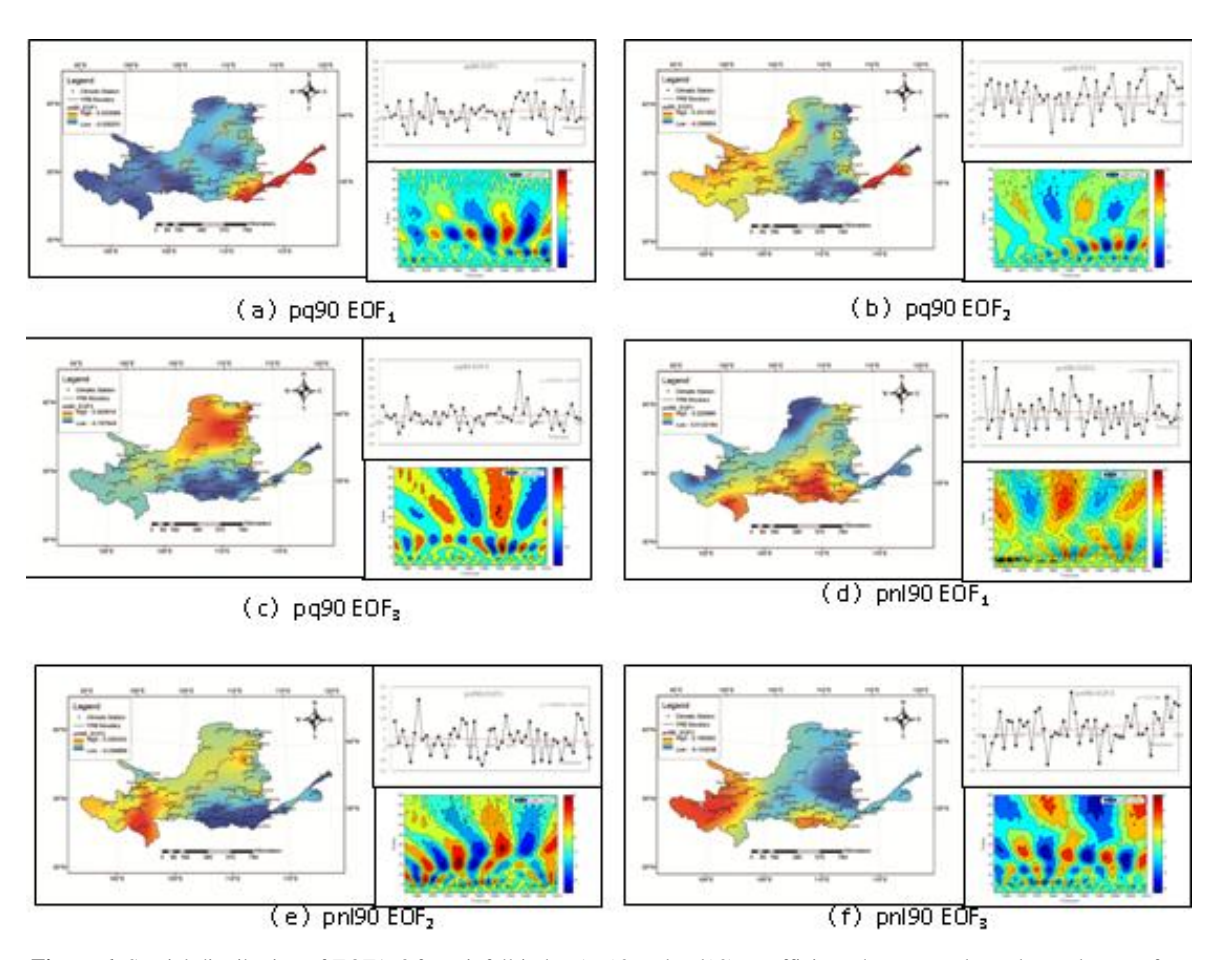


Figure 6. Spatial distribution of EOF1-3 for rainfall index (pq90 and pnl90), coefficient change trends, and wavelet transform of time series in the study area.

Wuhai and Wuyuan counties in the Inner Mongolia Autonomous Region to the north, and higher values in the south of the basin. The coefficient of EOF_2 decreased at a rate of 0.709/decade. It is also suggested that changes in tnq10 are generally larger than those of txq90, and changes in tnq10 are typically more than those in txq90. Over the whole time domain of tnq10, interannual cycles were evident with periods of 6, 21, and 37 years (EOF_1), 5 and 26 years (EOF_2), and 24 years (EOF_3), indicating the presence of well-developed interannual cyclicity throughout the period of wavelet analysis.

Table 4 and Figure 5 contain detailed descriptions of the indices tnfd and txhw90. For tnfd were 45.23, 14.86, and 7.39%, respectively, and their cumulative total variances were 45.23, 60.09, and 67.48%, respectively (Table 4). For txhw90, the cumulative total variances of EOF₁, EOF₂, and EOF₃ were 49.17, 61.06, and 67.81%, respectively, at the significant North level (North et al., 1982). The variances of EOF₁, EOF₂, and EOF₃ for tnfd were 49.17, 11.89, and 6.75%, respectively, and their cumulative total variances were 49.17, 61.06 and 67.81%, respectively. The spatial relationships of these three indices for EOF₁₋₃ are out-of-phase between the middle and northwest–southeast areas,

between the east and west areas, between the middle and west–east areas, and between the southwest and northeast areas. The regional decrease in tnfd occurred at the rapid rate of 31.166/decade. The value of tnfd followed a slightly decreasing trend before the late 20^{th} century, but decreased rapidly from then on. The trend lines of the coefficients of EOF_2 and EOF_3 showed a slight decrease and increase, respectively. The regional trends for EOF_2 and EOF_3 were -4.34/decade and 8.143/decade, respectively, and the positive values all occurred after 2000.

In addition, cycles with periods of 37 years, and 4 and 10 years, were observed in the wavelet analysis for EOF_1 and EOF_2 , respectively. The decrease of tnfd is in accordance with the increase of the temperature in winter in southern China (Ma and Fu, 2003). The analysis of the coefficient of the first, second and third principal components of txhw90 between 1961 and 2010 shows significant increasing trends at rates of 3.664/decade, 1.414/decade, and 1.071/decade, respectively. It appears that there is a tendency for high values of txhw90 to be concentrated over the middle, northwest, and southwest areas of the studied basin for three patterns. Over the whole time domain of txhw90, cycles with periods of 15, 6, and 14

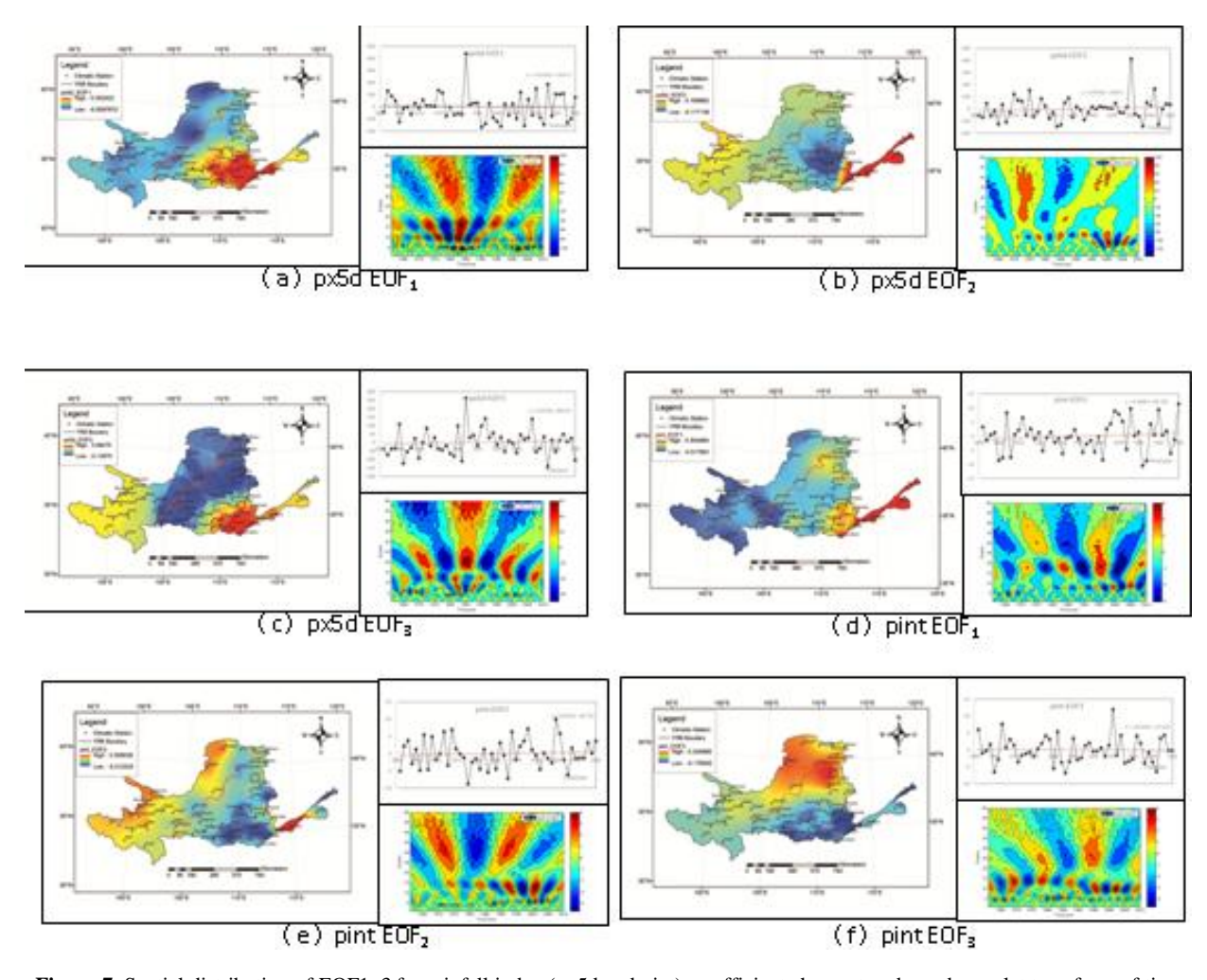


Figure 7. Spatial distribution of EOF1-3 for rainfall index (px5d and pint), coefficient change trends, and wavelet transform of time series in the study area.

years were recognized in the wavelet analysis for EOF_1 , EOF_2 , and EOF_3 , respectively.

Rainfall indices

Table 5 shows the 10 principal components of the indices of rainfall extremes. The results of the EOF analysis indicate that EOF1 to 10 are required to explain more than 68% of the total variance of the indices of rainfall extremes over the whole basin. EOF1 to 5 explained more than 48% of the total variance. Among them, the variance of the first, second, and third EOFs of the indices for rainfall extremes met the significant North level (North et al., 1982). This indicates that the spatial patterns of the EOFs for the indices of rainfall extremes are more complex than those for temperature extremes. It was found that the cumulative total variance of EOF1, EOF2, and EOF3 of the four indices of rainfall extremes were between 35.38 and 38.86% (Table 5), and that EOF1 explains 16.83, 21.21, 17.23 and 17.50% for pq90, pnl90, px5d, and pint, respectively. The plots of

the three EOFs that passed the significant North level are shown in Figure 6. Considering these results, it can be concluded that the distribution of rainfall extremes over most parts of the Yellow River Basin between 1961 and 2010 was not homogeneous. Various out-of-phase patterns of change occur for these EOFs over the basin. These results may be associated with broad-scale features of the monsoon circulation and its geographical variations.

As an example, for pq90 (Figures 6d to f) and 7 and Table 5), EOF $_1$ explains 16.83% of the total variance and exhibits an out-of-phase pattern between the southeast and northwest regions. Furthermore, high values of pq90 (Figure 6a) are concentrated over the southeast (downstream) of the study basin, while low values occur to the northwest (upstream). This means that the heavy rainfall threshold may increase in the southeast. The value of EOF $_2$ for pq90 exhibits an out-of-phase pattern between the middle and east–west areas. High values are concentrated over the east and west, with low values over the middle of the study area. The pattern for EOF $_3$ shows an

area of high values concentrated over the north of the Yellow River Basin, while low values are found to the south.

Figures 6d to f and 7 obtained from EOF analysis showed the patterns of the other three indices of rainfall extremes, which also have out-of-phase relationships; e.g., west and east, north and south, northeast and southwest. Trends and wavelet analysis of the time series of EOF1 to 3 (Figure 5) indicate that the significance of the trends in rainfall extremes is usually weaker than that of the trends in temperature extremes between 1961 and 2010, and also that the differences in the indices of rainfall extremes are most prominent. As a result, the wavelet analysis test results indicated that the EOF time series of the four indices of rainfall extremes showed prominent cyclical changes with periods of 5 to 7, 12 to 20, and 26 to 34 years.

Changes in run-off and its relationships with climate extreme indices

Motivated by the need to develop a better understanding of the intrinsic mechanism behind the changes in temperature and rainfall, the same trend detection procedure was conducted for the observed run-off from six hydrological stations at an annual timescale between 1961 and 2010 using linear regression and the M-K test. Compared with the indices of the climate extremes, observed run-off is a more complicated variable, and reflects the complex interactions among climate, vegetation, and soil characteristics, as well as, water supply. The observed run-off is sensitive to climate changes, such as variations in mean and extreme precipitation, and air temperature. The analysis of run-off data from six stations (at Lanzhou, Toudaoguai, Longmen, Sanmenxia, Huayuankou, and Lijin) over the period 1961 to 2010 showed a statically significant decrease (at the 95% level), with a particularly sharp decrease in the late 1980s (Figures 8 and 9). These results are in general agreement with the indices of the temperature and rainfall extremes indices. It is worth noting that the increasing trends in temperature and decreasing trends of some rainfall indices, over the study area are compatible with the results obtained from the observed run-off. However, the magnitudes of decrease in the numerical values of run-off were larger: up to 69, 83, 127, 196, 216, and 264 m³/s/decade between 1961 and 2010 for the Lanzhou, Toudaoguai, Longmen, Sanmenxia, Huayuankou, and Lijin stations, respectively. These results showed that run-off is enhanced by climate change, vegetation conditions, and other human activity.

Extreme temperature events result in higher evaporation rates, higher water vapor content, and consequently, an accelerated hydrological cycle. It is well established that climate change and run-off are closely related (Redmond and Koch, 1991). Table 6 presents the correlation coefficients between the observed run-off from the six

hydrological stations and the annual indices of temperature and rainfall extremes in the upper, middle, and lower regions. From the table, it can be seen that the temperature and rainfall extremes indices are closely related to the observed run-off. In general, the observed run-off was affected by climate change, human activity, land use, water resource development and utilization etc. The correlation coefficients between run-off and the four indices of temperature extremes, heavy rainfall days, and greatest 5-day rainfall are higher than those with the other rainfall indices in the upper and middle regions. At Lijin station, the coefficients between the observed run-off and the indices of temperature and rainfall extremes, except tng10 and tnfd, are less than those for the other stations. The results indicate that downstream run-off was affected more deeply by irrigation and abstraction than that in the upper and middle regions. Previous studies also indicated that climate change is the greatest contributor to observed changes in the water budget of the upper and middle reaches, while in the lower reaches river discharge is affected more by withdrawals for irrigation (Liu and Xia, 2004; Ma, 2005; Tang et al., 2008; Yang et al., 2008).

To confirm the aforementioned results, the anomalies of observed run-off from the six hydrological stations were compared with the climate extreme indices. Figure 6 shows the anomaly time series of the typically observed run-off from three stations and selected climate extreme indices. Figure 8a shows the time series of the annual anomalous txq90 and related plots for the periods 1961 to 2000 and 2001 to 2010, which are separated by the sharp change year at Toudaoguai station. From the figure, it can be seen that before 2000 the trends for txq90 and run-off differ; that is, txq90 was increasing at a rate of about 0.105°C/decade, while run-off was decreasing at a rate of about 109.2 m³/s/decade. After 2000, the increasing trend for txq90wa significant, at about 0.336°C/decade, and with a confidence level about 0.212, but the trend for run-off was considerable, at about 228.7 m³/s, and with a confidence level of about 0.834. The difference between the magnitude of the increasing and decreasing trends for txq90 and runoff suggests that the influence of climate and environmental change resulted in a statistically significant decrease in runoff. The present study focuses on northern China, which experienced rapid climate change, changes in land use and water use, and soil and water conservation measures. For the Huayuankou and Lijin stations, the trends in txg90 and run-off are fairly similar, and the effects of climate and the environment on observed run-off were negligible (Figure 8b and c). From Table 6 and Figure 6, it can be seen that climate was the main factor driving the decreasing trend in observed run-off.

Figure 9 also shows the time series of the annual anomalous typical indices, run-off, and related linear regression lines for the two periods separated by the sharp change. From the figure, it can be seen that the difference between the magnitude of the increasing and decreasing trends for different indices at different stations suggests

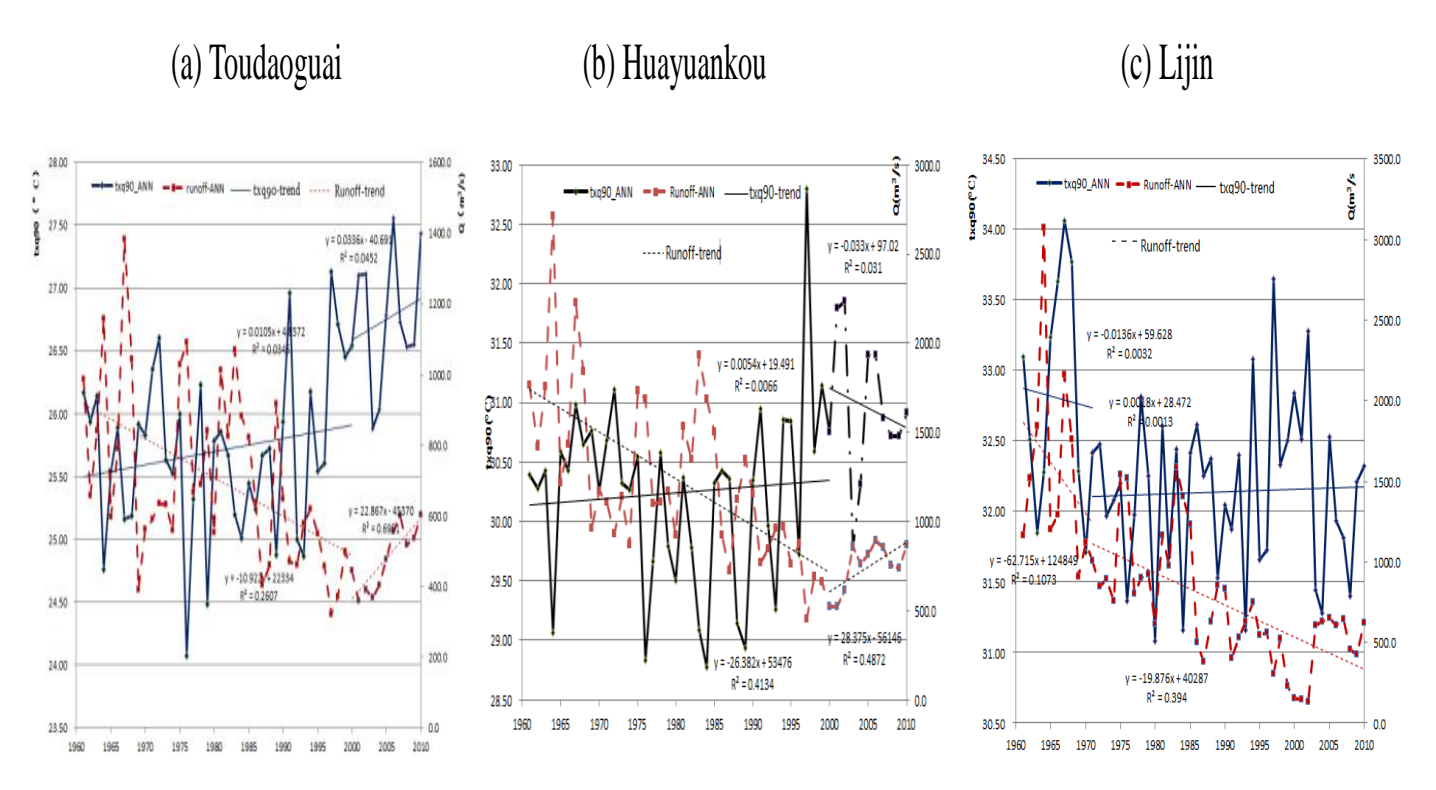


Figure 8. Annual time series of txq90 and run-off for the two periods, together with trend lines and related r^2 values for these variables at the Toudaoguai, Huayuankou, and Lijin stations.

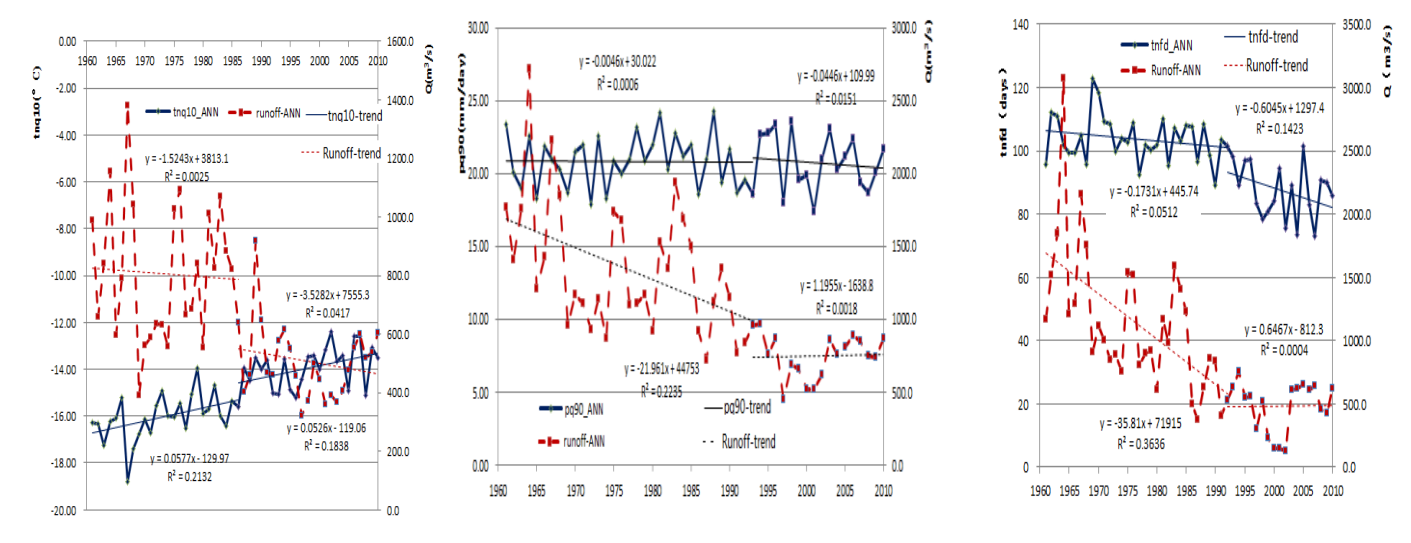


Figure 9. Annual time series of tnq10, pq90, tnfd, and runoff for the two periods, together with trend lines and related r^2 values for these variables at the Toudaoguai, Huayuankou, and Lijin stations.

that the climate extremes and environment change resulted in a decrease in run-off. From Table 6 and Figures 8 and 9, it can be seen that the decrease in run-off was caused by climate change, increased demands for water supply, land use change, etc. Taking water supply taken as an example of environmental change, over the period 1980 to 2010 (Table 7) water supply was 446.31, 415.80, and

 $485.11\times10^8~m^3$ in 1980, 1985, and 1990, respectively, and after 1990 water supply increased above $500\times10^8~m^3.$ The increasing trend in water supply exacerbated the decline in run-off. It is worth noting that interactions exist to some extent between the different individual indicators, with the increase of one extreme climate indicator depending on the decrease of another, and vice versa.

Upstream Midstream Downstream **Indices** Lanzhou Toudaoguai Longmen Huayuankou Sanmenxia Lijin txq90 0.4514** 0.5518^* 0.4073^* 0.4955^* 0.1572 0.4887 0.4931*** 0.4964*** 0.5389*** 0.5757*** 0.5161*** tnq10 0.5365*** 0.3392^{***} tnfd 0.2173 0.2827^{**} 0.3300^{**} 0.2877** 0.4743*** 0.4578^{***} 0.5099*** 0.4497^{***} 0.5057*** 0.5066^{***} txhw90 0.2078 0.2771** pq90 0.0640.103 0.2387^* 0.2769^{**} 0.1029 0.3731*** 0.3990*** 0.4579*** 0.5441*** pnl90 0.1803 0.1911 0.3900*** 0.3311** 0.4010^{***} 0.3510^{***} 0.3700^{***} px5d 0.1327 0.1109 0.1533 0.2466^* 0.2369^* 0.051 pint 0.2095

Table 6. Correlation coefficients between indices of climate extremes and runoff over the Yellow River Basin.

Table 7. Water supply in the Yellow River Basin for the period 1980–2010 (10⁸ m³).

V	Wate	er supply inner basin	Weden combode as and deafth a basin	Total		
Year	Surface water supply	Underground water supply	Total	Water supply to outside of the basin	Total	
1980	249.68	93.27	342.95	103.36	446.31	
1985	245.9	87.16	333.06	82.74	415.80	
1990	272.41	108.71	381.12	103.99	485.11	
1995	266.97	137.64	404.61	99.05	503.66	
2000	273.29	145.47	418.76	87.58	506.34	
2004	251.21	144.3	395.51	64.06	459.57	
2006	285.56	137.18	422.74	89.35	512.09	

Conclusions

This study examined spatial temporal changes in several indices related to climate extremes and observed run-off during the period 1961 to 2010 in the Yellow River Basin. Previous studies indicated that climate change is the greatest contributor to observed changes in run-off in the upper and middle reaches, while in the lower reaches river discharge is affected more by the development and utilization of water resources (Liu and Zhang, 2004; Ma, 2005; Tang et al., 2008). The change to a warmer climate is likely to generate higher temperatures and longer heat waves, while a shift to a drier climate leads to a decrease in run-off. As the analysis period (1961 to 2010) in this study was longer than that of previous studies (Zhang et al., 2008; Wang et al., 2012), it provides a more comprehensive analysis of both temporal and spatial trends in changing climate extremes.

During the study period (1961 to 2010), there was good agreement between changes in observed run-off and temperature indices, pnl90, and px5d, but this relationship was less well defined with the pq90 and pint indices (Table 6). For this region, the txq90, tnq10, and txhw90 indices increased by 0.6 to 1.3°C, 2.5 to 3.9°C, and 0.3 to 2.7 days, respectively, while tnfd decreased by 14.8 to 26.5

days for the period 1961 to 2010 at an annual scale. A significant upward trend in the high and low temperatures, and txhw90, but a downward trend for tnfd, was found at most stations in the Yellow River Basin. These changes contributed to a decreasing tendency in the observed runoff. Indices of rainfall extremes showed non-significant changes across the whole Yellow River Basin. Sharp changes in the indices of temperature extremes and in observed run-off occurred in the late 1980s and early 1990s, respectively.

Spatial variations in the temperature and rainfall indices were statistically significant. Out-of-phase patterns of varying annual temperature extremes were found between the north and south, west and east, and northwest and southeast of the basin. The spatial variation was more significant for the temperature extreme indices than that for rainfall indices. The decrease in the observed run-off showed significant relationships with the indices of temperature extremes, as well as, the pnl90 and px5d rainfall indices. It is important to note that changes in temperature, and some rainfall extremes, are closely related to evapotranspiration. Hence, the increase in temperature extremes has resulted in increased evapotranspiration, which has contributed to the observed run-off.

^{***, **,} and * indicate trends significant at the 99, 95, and 90% levels, respectively.

Conversely, changes in temperature and rainfall extremes have also affected the hydrological cycle. The increasing trends described for the txq90, tnq10, and hxtw90 indices, and the downward trends in tnfd, pnl90, and px5d, have contributed to the drier weather, which has resulted in the decrease in the observed run-off. Our results also showed that the shortage of water resources will become more pronounced in the Yellow River Basin with the increased occurrence of climate extremes. The results presented here will help to improve our understanding of the changes to climate extremes, and provide a basis for further investigation.

However, this study does not cover other climate indices, nor does it consider the influence of long-term climatic cycles that could be important in the interpretation of the observed trends. Therefore, it is recommended that further study is undertaken to determine the effects of regional climate (for example, multi-decadal oscillations) over different time spans and to assess its impact on run-off from the Yellow River Basin.

ACKNOWLEDGEMENTS

This research was funded by the National Natural Science Foundation of China (No. NSCF-51079131), the National Key Technology R and D Program (No. 2012BAB02B04-07), the Program for Innovative Research Team (in Science and Technology) at the University of Henan Province (IRTSTHN), and the CMA/Henan Key Laboratory of Agrometeorological Support and Applied Techniques. The authors are grateful to all colleagues and friends who have shared their meteorological and hydrological data with us and also all the reviewers for their insightful comments, which helped to improve the original draft of this paper.

REFERENCES

- Alexander L, Zhang X, Peterson T, Caesar J, Gleason B, Klein TA, Haylock M, Collins D, Trewin B, Rahimzadeh F (2006). Global observed changes in daily climate extremes of temperature and precipitation. J. Geophys. Res. Atmos. (1984-2012), 111, doi:10.1029/2005ID006290.
- Chen Y, Gao G, Ren GY, Liao YM (2005). Spatial and temporal variation of precipitation over ten major basins in China between 1956 and 2000. J. Nat. Res. 5:001.
- Chen Z, Xiang H, Gao R (2010). Trends of Ten Main Extreme Weather Indices in Wuhan. Adv. Clim. Change. Res. 6:22-28.
- Compagnucci RH, Blanco SA, Figliola MA, Jacovkis PM (2000). Variability in subtropical Andean Argentinean Atuel river; A wavelet approach. Environmetrics. 11:251-269.
- Di L, Scanlon BR, Fernando N, Meng L, Quiring SM (2012). Are Temperature and Precipitation Extremes Increasing over the U.S. High Plains?. Earth. Interact. 16:1-20.
- Ding T, Qian W, Yan Z (2010). Changes in hot days and heat waves in China during 1961–2007. Int. J. Climatol. 30:1452-1462.
- Easterling DR, Evans J, Groisman PY, Karl T, Kunkel KE, Ambenje P (2000a). Observed Variability and Trends in Extreme Climate Events: A Brief Review. Bull. Am. Meteorol. Soc. 81:417-425.
- Easterling DR, Meehl GA, Parmesan C, Changnon SA, Karl TR, Mearns LO (2000b). Climate extremes: observations, modeling, and impacts. Sci.

- 289:2068-2074.
- Emily IB, Huug VDD, Malaquias P (2013). Short-Term Climate Extremes: Prediction Skill and Predictability. J. Clim. 26(2):512-531.
- Frei C, Schär C (2001). Detection probability of trends in rare events: Theory and application to heavy precipitation in the Alpine region. J. Clim. 14:1568-1584.
- Fu G, Chen S, Liu C, Shepard D (2004). Hydro-climatic trends of the Yellow River basin for the last 50 years. Clim. Change. 65:149-178.
- Gemmer M, Fischer T, Jiang T, Su B, Liu LL (2011). precipitation extremes in the Zhujiang River basin, South China. J. Clim. 24:750-761.
- Hu Y, Maskey S, Uhlenbrook S (2012). Trends in temperature and rainfall extremes in the Yellow River source region, China. Clim. Change. 110:403-429.
- Hu Y, Maskey S, Uhlenbroo, S, Zhao H (2011). Streamflow trends and climate linkages in the source region of the Yellow River, China. Hydrol. Process. 25:3399-3411.
- Huang Y, Cai J, Yin H, Cai M (2009). Correlation of precipitation to temperature variation in the Huanghe River (Yellow River) basin during 1957-2006. J. hydrol. 372:1-8.
- Karl T, Easterling D (1999). Climate Extremes: Selected Review and Future Research Directions. Weather. Clim. Extreme. 42:309-325.
- Keiner LE, Yan XH (1997). Empirical orthogonal function analysis of sea surface temperature patterns in Delaware Bay, Geoscience and Remote Sensing. IEEE Transact. on. 35:1299-1306.
- Kendall M (1975). Rank Correlation Methods: Charles Griffin, London, UK. Klein TA, Können G (2003). Trends in indices of daily temperature and precipitation extremes in Europe, 1946-1999. J. Clim. 16:3665-3680.
- Labat D (2005). Recent advances in wavelet analyses: Part 1. A review of concepts. J. Hydrol. 314:275-288.
- Lee MA, Yeah CD, Cheng CH, Chan JW, Lee KT (2003). Empirical orthogonal function analysis of AVHRR sea surface temperature patterns in Taiwan Strait, J. Marine. Sci. Technol. 11:1-7.
- Li Z, Zheng Fl, Liu WZ, Flanagan DC (2010). Spatial distribution and temporal trends of extreme temperature and precipitation events on the Loess Plateau of China during 1961-2007. Quat. Int. 226:92-100.
- Liu C, Xia J (2004). Water problems and hydrological research in the Yellow River and the Huai and Hai River basins of China. Hydrological Proc. 18:2197-2210.
- Liu C, Zhang X (2004). Causal analysis on actual water flow reduction in the mainstream of the Yellow River. Acta Geographica Sinica. 59:323-330.
- Liu X (1999). Climatic characteristics of extreme rain-storm events in China, J. Catastrophol. 14:54-59.
- Ma Z, Fu C (2003). Interannual characteristics of the surface hydrological variables over the arid and semi-arid areas of northern China. Glob. Planet. Change. 37:189-200.
- Ma Z (2005). Historical regular patterns of the discharge in the Yellow River and the cause of their formation. Chinese J. Geophy. 48:1270-1275.
- Mann HB (1945). Nonparametric tests against trend, Econometrica. J. Econom. Soc. 245-259.
- Meddis R (1984). Statistics using ranks: a unified approach. Blackwell
- Meehl GA, Zwiers F, Evans J, Knutson T, Mearns L, Whetton P (2000). Trends in Extreme Weather and Climate Events: Issues Related to Modeling Extremes in Projections of Future Climate Change. Bull. Am. Meteorol. Soc. 81:427-436.
- Menael L, Bürger, G (2002). Climate change scenarios and runoff response in the Mulde catchment (Southern Elbe, Germany). J. hydrol. 267:53-64.
- Mohapatra M, Mohanty U, Behera S (2003). Spatial variability of daily rainfall over Orissa, India, during the southwest summer monsoon season, Int. J. Climatol. 23:1867-1887.
- North GR, Bell TL, Cahalan RF, Moeng FJ (1982). Sampling errors in the estimation of empirical orthogonal functions. Monthly. Weather. Rev. 110:699-706.
- Partal T, Kahya E (2006). Trend analysis in Turkish precipitation data. Hydrol. Proc. 20:2011-2026.
- Prokoph A, Patterson RT (2004). Application of wavelet and regression analysis in assessing temporal and geographic climate variability:

- Eastern Ontario, Canada as a case study. Atmosphere-Ocean. 42:201-212 Qin N, Chen X, Fu G, Zhai J, Xue X (2010). Precipitation and temperature trends for the Southwest China: 1960–2007. Hydrol. Proc. 24:3733-
- Redmond KT, Koch RW (1991). Surface climate and stream flow variability in the western United States and their relationship to large-scale circulation indices. Water. Resour. Res. 27:2381-2399.
- Ren G, Chen Y, Zou X, Zhou Y, Ren Y, Jiang Y, Ren F, Zhang Q, Wang X, Zhang L (2012). Change in climatic extremes over mainland China based on an integrated extreme climate index. Clim. Res. 50:113.
- Singh C (2004). Empirical Orthogonal Function (EOF) analysis of monsoon rainfall and satellite-observed outgoing long-wave radiation for Indian monsoon: a comparative study. Meteorol. Atmos. Phy. 85:227-234.
- Tang Q, Oki T, Kanae S, Hu H. Hydrological cycles change in the Yellow River basin during the last half of the twentieth century. J. Clim. 21:1790-1806.
- Villoria M, Scott E, Hoey T, Fischbacher-Smith D (2012). Temporal investigation of flow variability in Scottish rivers using wavelet analysis. J. Environ. Stat. 3:1-20.
- Vincent L, Aguilar E, Saindou M, Hassane A, Jumaux G, Roy D, Booneeady P, Virasami R, Randriamarolaza L, Faniriantsoa F (2011). Observed trends in indices of daily and extreme temperature and precipitation for the countries of the western Indian Ocean, 1961–2008. J. Geophy. Res. Atmos. (1984–2012), 116.
- Wang H, Yang Z, Saito Y, Liu JP, Sun X (2006). Interannual and seasonal variation of the Huanghe (Yellow River) water discharge over the past 50 years: connections to impacts from ENSO events and dams. Glob. Planet. Change. 50:212-225.
- Wang S, Li Y (2011). Channel variations of the different channel pattern reaches in the lower Yellow River from 1950 to 1999. Quat. Int. 244, 238-247.
- Wang W, Shao Q, Yang T, Peng S, Yu Z, Taylor J, Xing W, Zhao C, Sun F (2012). Changes in daily temperature and precipitation extremes in the Yellow River Basin, China. Stoch. Environ. Res. Risk. Assess. 27:401-421.
- Wang Z, Qian Y (2009). Frequency and intensity of extreme precipitation events in China. Adv. Water. Sci. 20:1-9.
- Xu CY, Singh V (2004). Review on regional water resources assessment models under stationary and changing climate. Water. Res. Management, 18:591-612.
- Xu Z, Zhang, N (2006). Long-term trend of precipitation in the Yellow River basin during the past 50 years. Geogr. Res. 25:27-34.
- Xu Z, Li J, Liu C (2007). Long-term trend analysis for major climate variables in the Yellow River basin. Hydrol. proc. 21:1935-1948.
- Yang T, Zhang Q, Chen YD, Tao X, Xu CY, Chen X (2008). A spatial assessment of hydrologic alteration caused by dam construction in the middle and lower Yellow River, China. Hydrol. proc. 22:3829-3843.
- Yang Z, Milliman J, Galle, J, Liu J, Sun X (1998). Yellow River's water and sediment discharge decreasing steadily, Eos. Trans. Am. Geophy. Union. 79:589-592.
- You Q, Kang S, Aguilar E, Pepin N, Flügel WA, Yan Y, Xu Y, Zhang Y, Huang J (2010). Changes in daily climate extremes in China and their connection to the large scale atmospheric circulation during 1961-2003. Clim. Dyn. 36:2399-2417.
- Yue S, Pilon P (2004). A comparison of the power of the t test, Mann-Kendall and bootstrap tests for trend detection. Hydrol. Sci. J. 49:21-37.
- Zhai P, Wang C, Li W (2007). A review on study of change in precipitation extremes. Adv. Clim. Change. Res. 3:144-148.
- Zhang Q, Xu CY, Yang T (2009). Variability of water resource in the Yellow River Basin of past 50 years, China. Water. Resour. Manag. 23:1157-1170.
- Zhang Q, Xu CY, Zhang Z, Ren G, Chen Y (2008). Climate change or variability? The case of Yellow river as indicated by extreme maximum and minimum air temperature during 1960–2004. Theor. Appl. Climatol. 93:35-43.
- Zhao F, Xu Z, Huang J (2007). Long-term trend and abrupt change for major climate variables in the upper Yellow River Basin. ACTA METEOROLOGICA SINICA-ENGLISH EDITION. 21:204.

Cite this article as:

Hu C, Chen J, Niu J, He F, Wang J (2016). Temporal and Spatial Changes in Climate Extremes and their Connection with Runoff in the Yellow River Basin between 1961 and 2010. Acad. J. Environ. Sci. 4(2): 020-038.

Submit your manuscript at http://www.academiapublishing.org/journals/ajes